Bioassay-guided Fractionation and Biological Activities of Antimycin A and 4-Hydroxybenzoic Acid Isolated from *Nocardiopsis* sp. Strain LC-9

Rozario Sagaya Jansi,[a] Ameer Khusro,[b,*] Paul Agastian,[c,*] Mikhlid H. Almutairi,[d] and Bader O. Almutairi [d]

Nocardiopsis sp. strain LC-9 was isolated from freshwater sediments and explored for its varied bioactive traits. Initially, ethyl acetate extract of strain LC-9 at varied concentrations showed pronounced antibacterial activities. After column chromatography, fraction F2 and F3 of the extract were identified as prominent fractions in terms of antimicrobial activities with low minimum inhibitory concentration values. Antioxidant activities of fraction F2 and F3 revealed remarkable scavenging of free radicals with low IC_{50} values (DPPH - 417.86 ± 0.24 µg/mL, ABTS - 431.6 ± 0.90 µg/mL, and FRAP - 404.36 ± 0.18 µg/mL). Fractions F2 and F3 were further characterized by UV spectrum, Fourier transform infrared spectroscopy, nuclear magnetic resonance, and liquid chromatography-mass spectrometry, and were identified as Antimycin A and 4-hydroxybenzoic acid. The compounds were further tested for anticancer activity against MCF-7 cells. The MTT assay showed reduced viability of MCF-7 cells with an increase in concentration of compounds. The IC_{50} values for Antimycin A and 4-hydroxybenzoic acid were 9.6 ± 0.7 µg/mL and 20.8 ± 0.4 µg/mL, respectively. Staining techniques confirmed the apoptosis mechanism. Finally, molecular docking (against targeted proteins of bacteria, fungus, and cancer cells) and molecular dynamics confirmed the pharmaceutical efficacy of the purified compounds.

DOI: 10.15376/biores.19.4.7673-7697

Keywords: Nocardiopsis sp.; Antimycin A; 4-Hydroxybenzoic acid; MCF-7; Molecular docking; Molecular dynamics

Contact information: a: Department of Bioinformatics, Stella Maris College, Chennai-600086, Tamil Nadu, India; b: Department of Research Analytics, Saveetha Dental College and Hospitals, Saveetha Institute of Medical and Technical Sciences, Saveetha University, Chennai – 600077, India; c: Research Department of Plant Biology and Biotechnology, Loyola College, Chennai-600034, Tamil Nadu, India; d: Department of Zoology, College of Science, King Saud University, P.O. Box 2455, Riyadh 11451, Riyadh, Saudi Arabia;
**Corresponding author: armankhan0301@gmail.com; agastianloyolacollege@gmail.com*

INTRODUCTION

Research in discovering actinomycetes and screening their biological activity is a major field of interest in India. Over the past three decades, actinomycetes have substantiated themselves as dependable sources of therapeutically useful bioactive metabolites (Saraswathi *et al*. 2020). The compounds display a comprehensive scale of bioactivities, such as antimicrobial, anticancer, cytotoxic, neurotoxic, antiviral, and antineoplastic activities (Selim *et al*. 2021).

It has been reported that of the entire microbial metabolites in the globe, 70% is contributed by actinomycetes, while 20% by fungi, 7% by *Bacillus* sp., and 1 to 2% by *Pseudomonas* sp. This substantiates that actinomycetes stand out exclusively in the production of an array of biologically active metabolites for clinical research (Hauhan and Gohel 2020).

Of the antibiotic-producing microorganisms, actinomycetes still remain the major constituent of diverse bioactive and pharmaceutically distinct metabolites. Different classes of antibiotics with varying target mechanisms and unique mode of action, such as amino-glycosides, polyketides, chloramphenicols, tetracyclines, *etc.*, are produced by the class Actinobacteria. Molecular data, such as 16S rRNA sequencing, have been beneficial in actinomycetes classification and identification (Salwana and Sharma 2020).

Soil inhabiting *Nocardiopsis* sp. belongs to the phylum Actinobacteria, containing a large repository of unique bioactive compounds. The genus *Nocardiopsis* (Nocardiopsaceae) was first defined by J. Meyer in 1976. Morphological characters, phylogeny, and chemotaxonomic properties of the species articulate a discrete ancestry from the order 'Actinomycetales'. This genus comprises of Gram positive aerobic actinomycetes with aerial mycelium that fragments into spores and form wrinkled/folded colonies on organic media (Abdel-Razek *et al*. 2020; Dror *et al*. 2020)

Nocardiopsis is reported to contain 24 species and two subspecies, mostly thriving in alkaliphilic or halophilic environments. The prominent features of the cell wall of this genus include: meso-2,6-diaminopimelic acid (cell-wall chemotype III), phosphatidyl-choline as a characteristic phospholipid (phospholipid type III), menaquinones, absence of madurose and nocardomycolic acids, and novel teichoic acid compositions. The members of this species generally have genomes with a high load of G+C (64 to 71%) composition (Ngema *et al*. 2023). *Nocardiopsis* spp. are reported in diverse regions including saline, hypersaline, desert, and alkaline environments (Ramalingam *et al*. 2022; Kumar *et al*. 2023).

Microbial metabolites account for 45% of the world market of pharmaceuticals. The marketing of the different classes of products reaches millions of dollars each year. In recent times, discovery of novel compounds with bioactive potential has become rare and remains a great challenge. This provokes recent researchers to find new species (genera or families) with altered and novel genes to produce distinct metabolites of new purpose. In this investigation, a significant attempt was undertaken to assess the biological activities of bioactive metabolites isolated from *Nocardiopsis* sp. strain LC-9.

EXPERIMENTAL

Sample Site, Sampling Procedure, and Isolation

Freshwater soil sediments were collected from Chembarambakkam lake at a latitude of 13° 00' 41.69" N and longitude of 80° 03' 38.27" E Chennai, Tamil Nadu, India. Actinomycetes were isolated from the collected soil samples using serial dilution technique on Actinomycetes Isolation Agar (AIA) medium augmented with actidione (20 mg/L) and nalidixic acid (100 mg/L). Plates were incubated at 28 ± 2 °C for 7 to 10 days. After the required incubation period, pure culture of isolates was obtained using the streaking method and stored at 4 °C (Fig. 1).

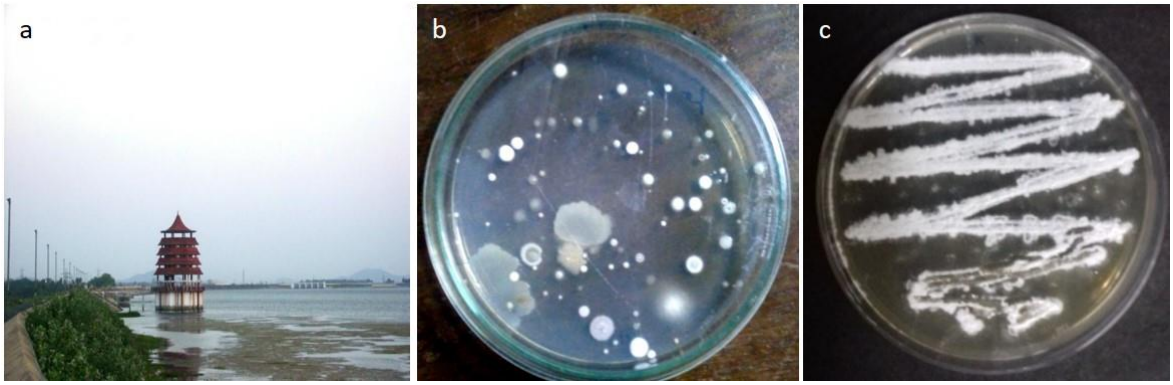

Fig. 1. a) Freshwater soil sediments collection site (Chembarambakkam lake), b) Actinomycetes colonies isolated on AIA medium using serial dilution method, and c) Pure culture of isolate

Preliminary Screening by Perpendicular Streak Method

Primary screening was performed by the cross-streak method on Mueller Hinton Agar media against 11 bacterial pathogens. This was done by inoculating a single streak of the pure culture of isolates in the center of the Petri plates and stored at 28 ± 2 °C for 5 days. Successively, the test pathogens were streaked at 90° angle and incubated at 37 °C overnight. Lack of growth of pathogens indicates antibacterial activity of isolates.

Morphological and Molecular Characterization of Potent Isolate

Morphological and cultural features of the potent isolate was observed by inoculating and incubating the culture in various media including AIA, MNGA, SCA, NA, M5, ISP1, ISP2, ISP3, and ISP4 aseptically at 28 °C for 7 to 14 days. The isolate was subjected to smear preparation for Gram staining. The spore chain characteristic of the selected isolate was observed by scanning electron microscopy (SEM; JSM5600LV, JEOL, Japan). For efficient genomic DNA isolation, Hipura Streptomyces DNA Purification Kit (Hi-media, India) was used. DNA was eluted and visualized by 1% agarose gel electrophoresis. Polymerase chain reaction (PCR) amplification was performed using the following universal primers: 27F (5`AGTTTGATCCTGGCTCAG3`) and 1492R (5`ACGGCTACCTTGTTACGACTT3`). Sequencing was achieved using Applied Biosystems, (Foster City, CA) USA, and the standard quality of the sequence was checked using sequence Scanner Software v1 (Applied Biosystems, Foster City, CA, USA). Similarly, the sequence alignment and editing were carried out by Geneious Pro v5.6 (http://www.geneious.com). Finally, a phylogenetic tree was constructed using MEGA X software (https://www.megasoftware.net/) for the target sequence.

Antibacterial Activity of Crude Extract

The isolate was inoculated into modified nutrient glucose broth medium and allowed to ferment for 7 days at 28 °C at 180 rpm. After fermentation, the culture filtrates were extracted by liquid-liquid extraction method using ethyl acetate. Antibacterial activity of the extract at varied concentrations (1.25 to 5 mg/mL) was tested using the disc diffusion method. Streptomycin was used as a positive control.

Bioactive Metabolites Extraction by Column Chromatography

The crude ethyl acetate extract was separated by silica gel column (4.5 to 60 cm) chromatography. A total of 10 g of the extract were used for the column preparation along with silica gel (65 to 70 g). The column initially used ethyl acetate and was gradually added

with increasing the polarity mixtures of solvents of hexane and ethyl acetate (0 to 100%). Four fractions (F1, F2, F3, and F4) were collected at regular intervals and spotted in TLC plates with the same solvent proportion to find the Retention factor (Rf) values. Concurrently, fractions with the same Rf values were combined and evaporated to remove the solvents at appropriate conditions.

Minimum Inhibitory Concentration (MIC) Determination

The collected fractions were tested for antimicrobial activity against 11 bacterial pathogens [*Bacillus subtilis* (MTCC 441), *Staphylococcus aureus* (ATCC 25923), MRSA Clinical pathogen (15DR), *S. aureus* (Methicillin sensitive), *Enterobacter faecalis* (MTCC 29212), *Escherichia coli* (MTCC 40), *Klebsiella pneumoniae* (MTCC 109), *Enterobacter aerogenes* (MTCC 111), *Vibrio parahaemolyticus* (MTCC 451), *Yersinia enterocolitica* (MTCC 840), and *Pseudomonas aeruginosa* (ATCC 15380)] and 5 fungal cultures [*Aspergillus flavus* (MTCC 9390), *Aspergillus niger* (MTCC 478), *Botrytis cinerea* (MTCC 359), *Candida albicans* (MTCC 227), and *Candida lunata* (MTCC 2098)] *via* the microdilution method (Venkatadri *et al*. 2017). All the pathogens were obtained from Entomology Research Institute, Loyola College, Chennai, India. Standard streptomycin and fluconazole were used as bacterial and fungal positive control, respectively.

Antioxidant Properties of Active Fractions

The DPPH (2, 2, diphenyl-1-picryl hydrazyl) radical scavenging, ABTS [2, 2'-azinobis (3-ethylbenzothiazoline-6-sulfonic acid)] radical scavenging, FRAP (ferric reducing antioxidant power) activity, and total reducing power assay of the most active fractions (F2 and F3) were determined as per the methodology of Oyaizu (1986), Benzie and Strain (1996), Jia *et al*. (1999), Kekuda *et al*. (2010), and Prasathkumar *et al*. (2021). The IC_{50} values were calculated by online linear regression curve.

Structure Elucidation of Active Fractions

Based on the antimicrobial and antioxidant results of fractions, fraction F2 and F3 were selected and further characterized by UV spectrum (JASCO, model V-750, Japan), Fourier transform infrared (FT-IR) spectrum (Bruker, Alpha-T ATR-FTIR Spectrometer model, TENSOR 27, Germany) with the spectra characteristics detected at 20000 to 500 cm^{-1} range, ^{1}H and ^{13}C nuclear magnetic resonance (NMR) (Bruker, model AVANCE III 500 NMR, Germany), and liquid chromatography-mass spectrometry (LC-MS).

Cytotoxicity Assay of Isolated Compounds

In vitro cytotoxic activity of the compounds was tested against human breast cancer cell line (MCF-7) procured from the National Center for Cell Sciences (NCCS), Pune, India. The cells were incubated at 37 °C with 5% CO_2 in a humidified CO_2 chamber. The cytotoxicity was determined using MTT [3-(4,5- dimethylthiazol-2-yl)-2,5-diphenyl-tetrazolium bromide] assay as per the methodology of Mosmann (1983). The percentage of viability was calculated as:

$$\% \text{ viability} = [\text{Absorbance of sample}/\text{Absorbance of control}] \times 100$$

Apoptotic Cell Death Analysis

The apoptotic cells were observed by staining the cells with 1 µL of 100 mg/mL of acridine orange (AO) and 100 mg/mL of ethidium bromide (EtBr) in distilled water. To

this, 90 µL of cell suspension (1×10^5 cells/mL) were added. Finally, after staining with 10 µL of DAPI (4′, 6-diamidino-2-phenylindole), the samples were observed under fluorescent microscope (Nikon Eclipse, Inc. Tokyo, Japan) (Clarance *et al*. 2020).

Molecular Docking Analysis and ADME Prediction

N-myristoyl transferase (1IYL) and 14-α-demethylase (5FSA) were used as targeted proteins for fungi. Dihydropteroate synthetase (2VEG), Isoleucyl- tRNA Synthetase (1ILE), Alanine racemase (2RJG), Penicillin-binding protein 1a (3UDI), and Dihydrofolate Reductase (3SRW) were used as targeted proteins for bacteria. In contrast, vascular endothelial growth factor receptor 2 (5EW3), B-cell lymphoma 2 (5VAX), DNA topoisomerases II (1ZXM), HER2-human epidermal growth factor receptor 2 (5O4G), and EGFR (Epidermal Growth Factor Receptor; 2J6M) were used as targeted proteins of cancer cell line. Docking was performed between the compound and selected proteins using Schrödinger software (version 2020-1; Maestro, Schrödinger, LLC, New York, NY, USA). The ADME (absorption, distribution, metabolism, and excretion) likelihood was estimated using the Qik prop tool to evaluate the lead likeliness and Lipinski violations.

Molecular Dynamics (MD) Simulations

Molecular dynamics simulations were run by Desmond v3.6 Package (Schrödinger, New York, NY, USA) to determine the stable conformation of the protein-ligand complex and effectiveness of the compound against the target protein. The studies were performed for 100 ns simulation to determine the interactions and calculate the Root Mean Square Deviation (RMSD), Root Mean Square Fluctuation (RMSF), and contact points.

Statistical Analysis

All the experiments were performed in triplicate and results were recorded as Mean ± SD. ANOVA was used to analyze the statistical significance and values with $P \leq 0.05$ were considered significant.

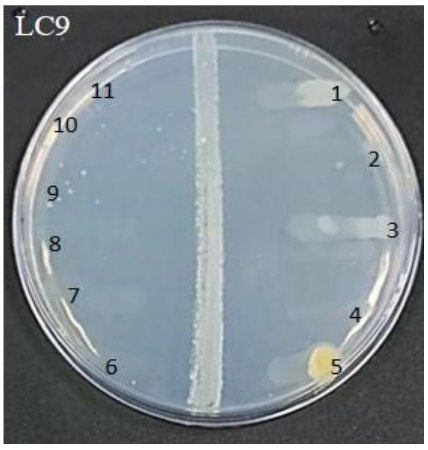

Fig. 2. Screening for antibacterial activity of isolate LC-9. The isolate showed inhibition of pathogen growth. 1 – *B. subtilis* (MTCC 441), 2 – *S. aureus* (ATCC 25923), 3 – MRSA Clinical pathogen (15DR), 4 – *S. aureus* (Methicillin sensitive), 5 – *E. faecalis* (MTCC 29212), 6 – *E. coli* (MTCC 40), 7 – *K. pneumoniae* (MTCC 109), 8 – *E. aerogenes* (MTCC 111), 9 – *V. parahaemolyticus* (MTCC 451), 10 – *Y. enterocolitica* (MTCC 840), 11 – *P. aeruginosa* (ATCC 15380).

RESULTS AND DISCUSSION

Screening and Identification of *Nocardiopsis* sp.

Figure 2 illustrates primary screening for antibacterial activity of isolate LC-9. Results showed that the growth of all the tested bacterial pathogens (horizontally streaked towards the circumference of the petriplate) was inhibited in the presence of isolate LC-9 (longitudinally streaked at the center of the petriplate), indicating prominent antibacterial activity of isolate LC-9.

Further, the morphological characteristic of isolate LC-9 by Gram staining and SEM analysis showed aerial mycelium and hyphae of various lengths (Fig. 3).

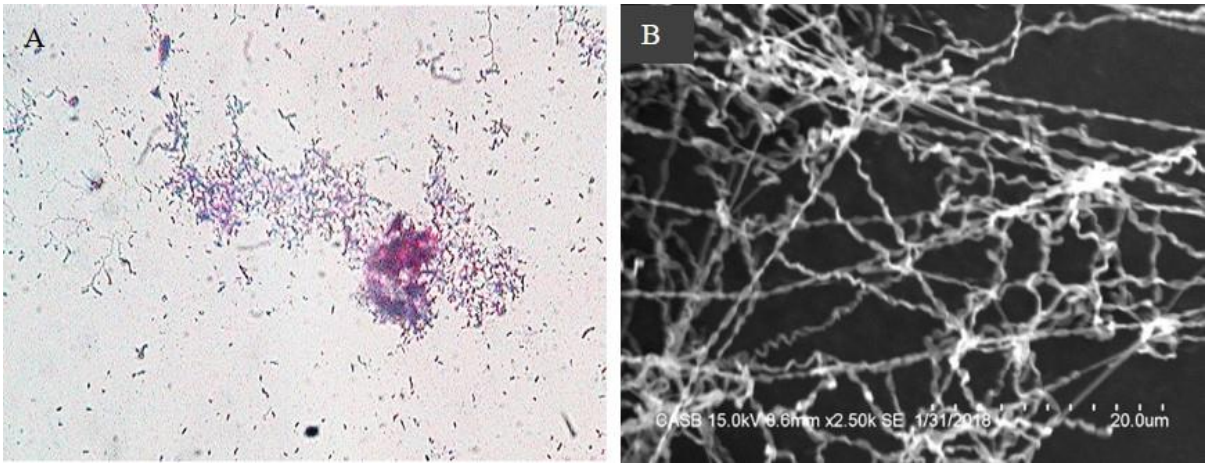

Fig. 3. A) Gram staining and B) SEM analysis of isolate LC-9

Molecular characterization, followed by phylogenetic tree analysis indicated that the isolate belonged to the genus *Nocardiopsis*, and the strain was designated as *Nocardiopsis* sp. strain LC-9 (Accession No. - MH266471). The optimal tree with the branch length of 499.08910173 is shown in Fig. 4. The tree was inferred from bootstrap consensus analysis (100 replicates) with a total of 1535 positions.

The genus *Nocardiopsis* from Actinobacteria plays a significant role in the production of secondary metabolites, especially of pharmacological importance. They thrive in extreme environments with high metabolic activity, thereby withstanding and resisting attacks of other pathogens. Several studies showed that extracts of *Nocardiopsis* have the capability to produce natural products with unveiled cytotoxic (Siddharth *et al*. 2021) and antimicrobial competence (Goel *et al*. 2021).

Ethyl acetate extract of strain LC-9 presented potential antibacterial activity against the test pathogens. The extract at 5 mg/mL concentration revealed a maximum zone of inhibition of 18.5 ± 0.16, 18.5 ± 0.28, 18.16 ± 0.57, 17.5 ± 0.28, and 17.16 ± 0.88 mm against *B. subtilis*, *Y. enterocolitica*, *V. parahaemolyticus*, *E. aerogenes*, and *S. aureus* (Methicillin sensitive), respectively (Table 1).

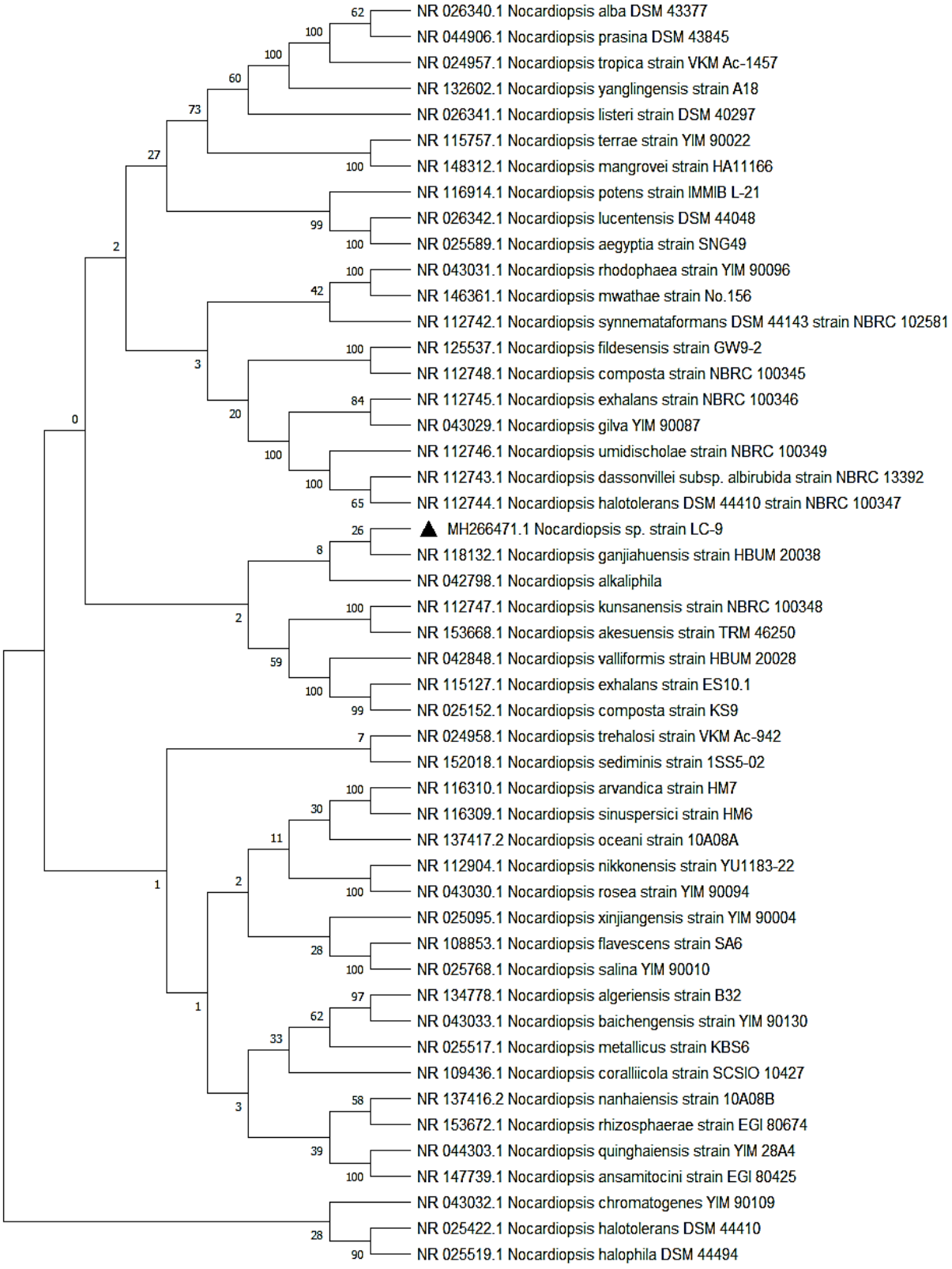

Fig. 4. Phylogenetic tree of strain LC-9

Antibacterial Activity of Strain LC-9 Extract

Table 1. Antibacterial Activity of Ethyl Acetate Extract of Strain LC-9

Bacterial Strains	1.25 (mg/mL)	2.5 (mg/mL)	5 (mg/mL)	Streptomycin
Gram Positive Bacteria				
B. subtilis (MTCC 441)	-	16.33 ± 0.5^{b}	18.5 ± 0.16^{a}	15.16 ± 0.72^{c}
S. aureus (ATCC 25923)	-	-	16.21 ± 0.72^{a}	15.5 ± 0.28^{b}
MRSA Clinical pathogen (15DR)	14.83 ± 1.01^{b}	12.33 ± 1.16^{d}	16.33 ± 0.33^{a}	13.83 ± 0.44^{c}
S. aureus (Methicillin sensitive)	-	14.67 ± 0.88^{b}	17.16 ± 0.88^{a}	11.83 ± 1.01^{c}
E. faecalis (MTCC 29212)	-	-	16.36 ± 0.57^{a}	11.5 ± 0.28^{b}
Gram Negative Bacteria				
E. coli (MTCC 40)	-	14.33 ± 0.6^{b}	15.16 ± 0.33^{a}	12.5 ± 0.28^{c}
K. pneumoniae (MTCC 109)	-	15.66 ± 0.44^{b}	16.33 ± 1.16^{a}	14.83 ± 0.44^{c}
E. aerogenes (MTCC 111)	-	15.33 ± 0.33^{b}	17.5 ± 0.28^{a}	9.16 ± 0.44^{c}
V. parahaemolyticus (MTCC 451)	-	-	18.16 ± 0.57^{a}	13.3 ± 0.33^{b}
Y. enterocolitica (MTCC 840)	-	14.3 ± 0.5^{b}	18.5 ± 0.28^{a}	13.17 ± 0.16^{c}
P. aeruginosa (ATCC 15380)	-	-	15.83 ± 1.15^{a}	15.8 ± 0.28^{a}

Each value represents the mean ± SD of triplicate experiments. ^{abcd}Values are significantly different (P<0.05). '-': Indicates lack of antibacterial activity.

MIC Determination of Strain LC-9 fractions

Among 4 fractions tested, fraction F2 of strain LC-9 exhibited promising antimicrobial activities against the indicator pathogens with minimum MIC value of 15.625 µg/mL (against MRSA clinical pathogen and *K. pneumoniae*) and 31.25 µg/mL (against *Curvularia lunata*). Likewise, fraction F3 showed potential MIC value of 31.25 µg/mL against MRSA clinical pathogen, *S. aureus* (Methicillin sensitive), *K. pneumoniae*, *V. parahaemolyticus*, *Y. enterocolitica*, and *Aspergillus niger* (Table 2).

Antioxidant Activity of Strain LC-9 Fractions

Antioxidant activities of fractions F2 and F3 are shown in Fig. 5. With increasing concentration (200 to 1000 µg/mL), the fractions showed approximately 38 to 80% of scavenging activities compared to the standards. IC_{50} values of fraction F2 were estimated as 417.86 ± 0.24, 431.6 ± 0.90, 404.36 ± 0.18, and 416.16 ± 1.54 µg/mL towards DPPH scavenging, ABTS scavenging, FRAP assay, and total reducing power assay, respectively. In contrast, IC_{50} values of fraction F3 were estimated as 321.72 ± 0.18, 333.71 ± 1.54, 414.67 ± 1.36, and 401.67 ± 1.39 µg/mL towards DPPH scavenging, ABTS scavenging, FRAP assay, and total reducing power assay, respectively.

Table 2. MIC Values of Fractions (F1, F2, F3, and F4)

Test Pathogens	MIC (µg/mL)				
	F1	F2	F3	F4	Standard
Gram Positive Bacteria					
B. subtilis (MTCC 441)	-	> 62.5	> 125	-	> 15.625
S. aureus (ATCC 25923)	-	> 31.25	> 62.5	> 15.625	> 62.5
MRSA Clinical pathogen (15DR)	-	> 15.625	> 31.25	-	> 125
S. aureus (Methicillin sensitive)	-	> 62.5	> 31.25	-	> 62.5
E. faecalis (MTCC 29212)	-	> 125	> 62.5	> 31.25	> 125
Gram Negative Bacteria					
E. coli (MTCC 40)	-	> 62.5	> 125	-	> 250
K. pneumoniae (MTCC 109)	-	> 15.625	> 31.25	-	> 250
E. aerogenes (MTCC 111)	-	> 125	> 125	-	> 125
V. parahaemolyticus (MTCC 451)	-	> 125	> 31.25	-	> 62.5
Y. enterocolitica (MTCC 840)	> 31.25	> 62.5	> 31.25	-	> 62.5
P. aeruginosa (ATCC 15380)	-	> 125	> 250	-	> 125
Fungal Cultures					
Aspergillus flavus (MTCC 9390)	> 31.25	> 62.5	> 125	-	> 25
A. niger (MTCC 478)	-	> 62.5	> 31.25	-	> 62.5
Botrytis cinerea (MTCC 359)	-	> 125	> 62.5	-	> 62.5
Candida albicans (MTCC 227)	-	> 62.5	> 125	-	> 15.625
C. lunata (MTCC 2098)	-	> 31.25	> 125	> 31.25	> 25

'-': No activity

Characterization of fraction F2 and F3

The UV spectrum of the fraction F2 (compound 1) showed peak at 219 to 226 nm (Fig. 6A). Similarly, the FT-IR spectrum at 3419 cm^{-1} revealed the presence of O-H or N-H groups. The peak at 2927 to 2974 cm^{-1} showed C-H stretching in $-CH_3$ or $-CH_2$. The peak at 1746 cm^{-1} described the C=O stretching, peak at 1534 to 1540 cm^{-1} indicated the presence of C-O-C of aromatic ring, and the peak at 1050 cm^{-1} specified alkyl group (Fig. 6B).

The ^1H NMR spectra of compound 1 had the following spectrum: at 0.874 ppm is the (3H, t), 1.116 to 1.207 ppm (2H, m), 1.305 to 1.318 ppm (3H, d), 2.493 to 3.326 ppm (CH_3, 3H, s), 4.856 to 4.996 ppm (aromatic, 1H, m), 5.311 to 5.342 ppm (aromatic, 1H, d), 5.565 to 5.618 ppm (aromatic, 1H, d), 6.901 to 6.931 (NH, 1H, d), 7.870 to 7.854 (NH, 1H,

d), 8.237 to 8.326 ppm (CHO, 1H, d), 12.765 ppm (OH, 1H, s), respectively. The ^{13}C NMR spectra showed the presence of methyl (CH_3) group in the upfield region between 39.538 and 40.540 ppm. The splitting patterns of both the NMR studies designated good evidence that compound 1 was identified as Antimycin A (Fig. 7A and 7B). Through the mass spectrum, the molecular weight (549.28 g/mol) and molecular formula ($C_{28}H_{40}N_2O_9$) of the compound were deduced in the study. The structure of the compound was elucidated and predicted to be Antimycin A of the subtype Antimycin A_{1ab} (Fig. 8).

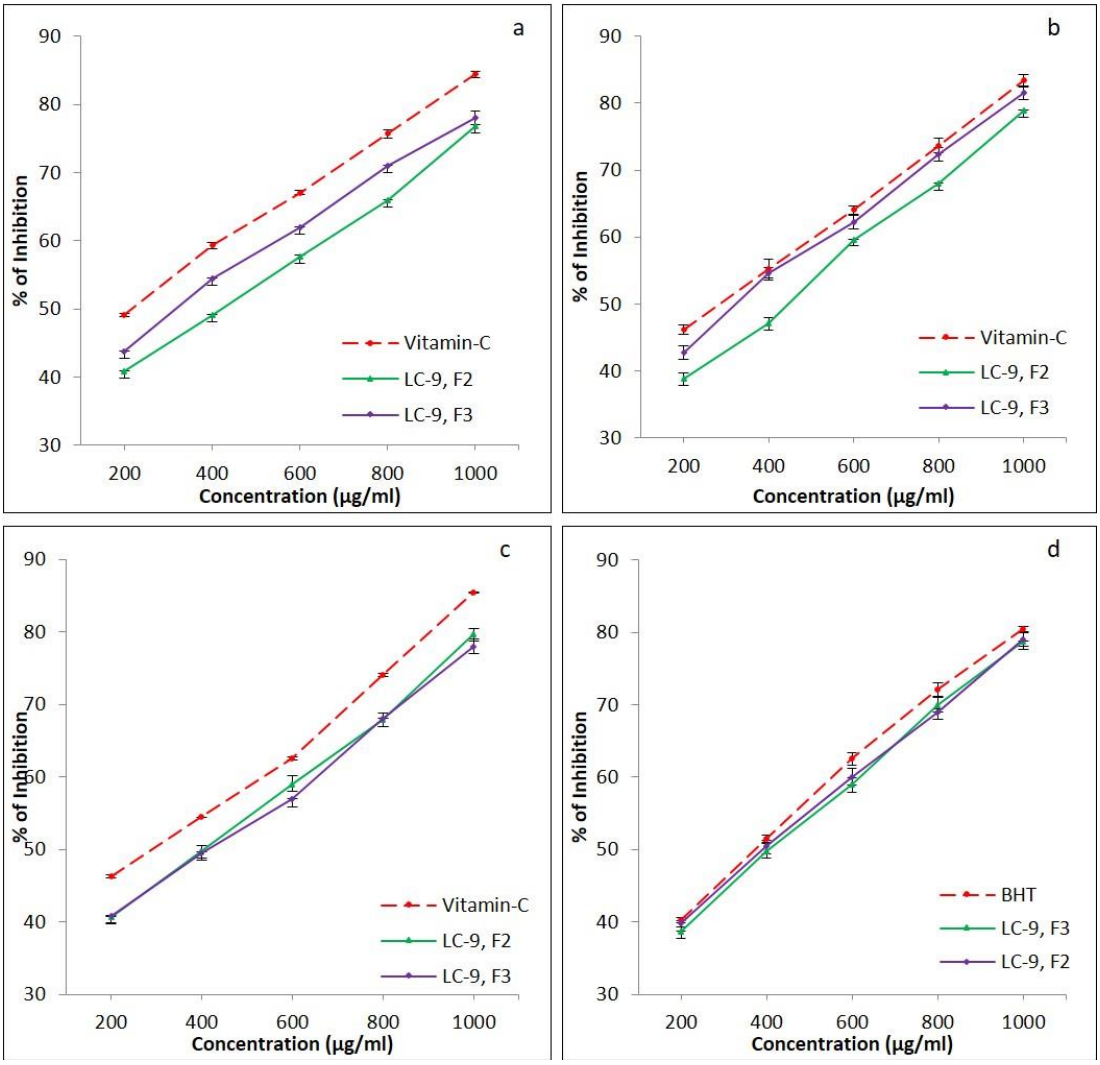

Fig. 5. a) DPPH, b) ABTS, c) FRAP, and d) Total reducing power activity of standard and fractions (F2 and F3) at varied concentrations. Each value presents the mean ± SD of triplicate experiments.

Antimycin A is an antibiotic made of nine-membered dilactone ring. In 1949, it was first isolated and categorized as a fungicide from *Streptomyces* sp. (Han *et al*. 2012). So far, more than 20 Antimycin A derivatives have been reported. Class of Antimycin compounds generally express antibacterial and antifungal properties due to the presence of biosynthetic gene clusters like non-ribosomal peptide synthetases (NRPSs) and polyketide synthases (PKSs) in actinomycete strains. Detection methods like PCR amplification (for

PKSs and NRPSs genes), NMR, and LC-MS were used to identify and categorize the different types of antimycin (Hytti *et al*. 2019).

Antimycin A plays an important role in the electron transport chain by inhibiting complex III. It also increases cell death and is the reason for the downfall of oxidative phosphorylation (Kauppinen 2018). In this study, Antimycin A isolated from strain LC-9 showed good antimicrobial and high antioxidant potential. Previously, two novel antimycins, Urauchimycins A and B, were obtained from *Streptomyces* sp. strain Ni-80, which showed antifungal activity against *C. albicans*. Likewise, there was an effective antifungal activity of Antimycins A_{19} and A_{20} from *S. antibioticus* H74-18 against *C. albicans*. Wherein, Antimycin B2 from *S. lusitanus* XM52 showed antibacterial activity against *S. aureus* and *L. hongkongensis* (Imamura *et al*. 1993; Han *et al*. 2012).

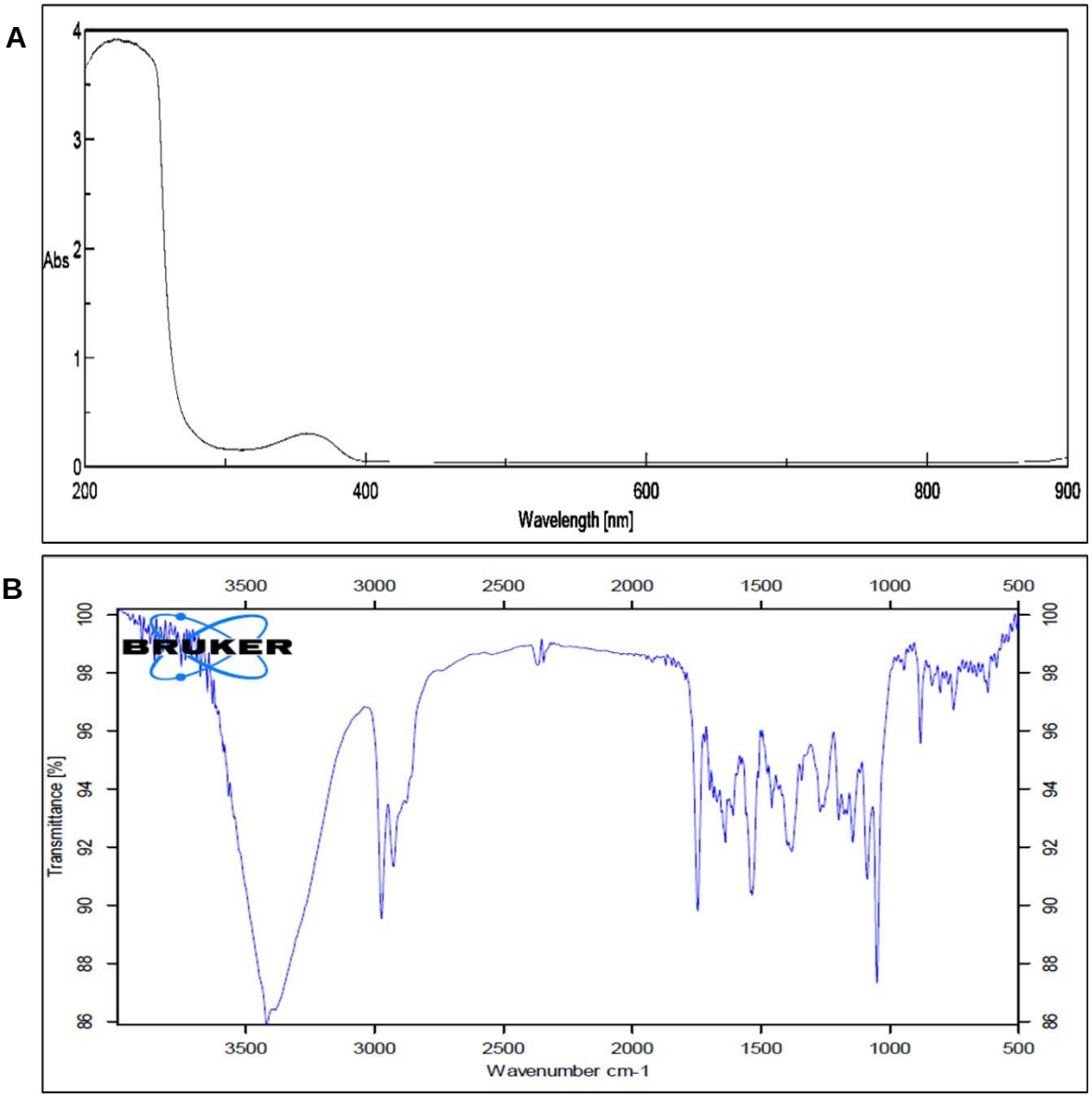

Fig. 6. A) UV visible spectroscopy and B) FT-IR spectroscopy of Antimycin A

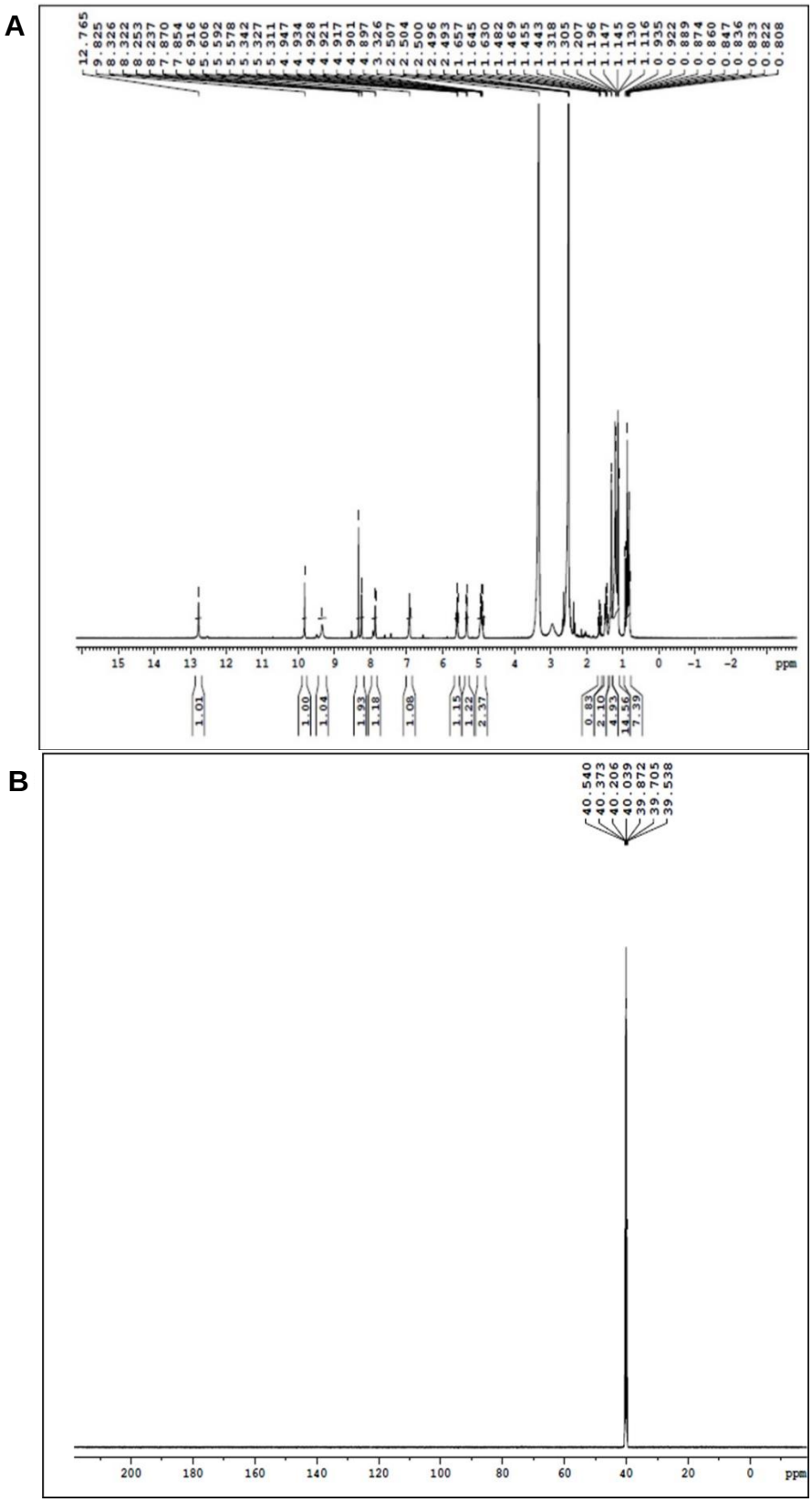

Fig. 7. A) ^{1}H NMR spectrum and B) ^{13}C NMR spectrum of Antimycin A

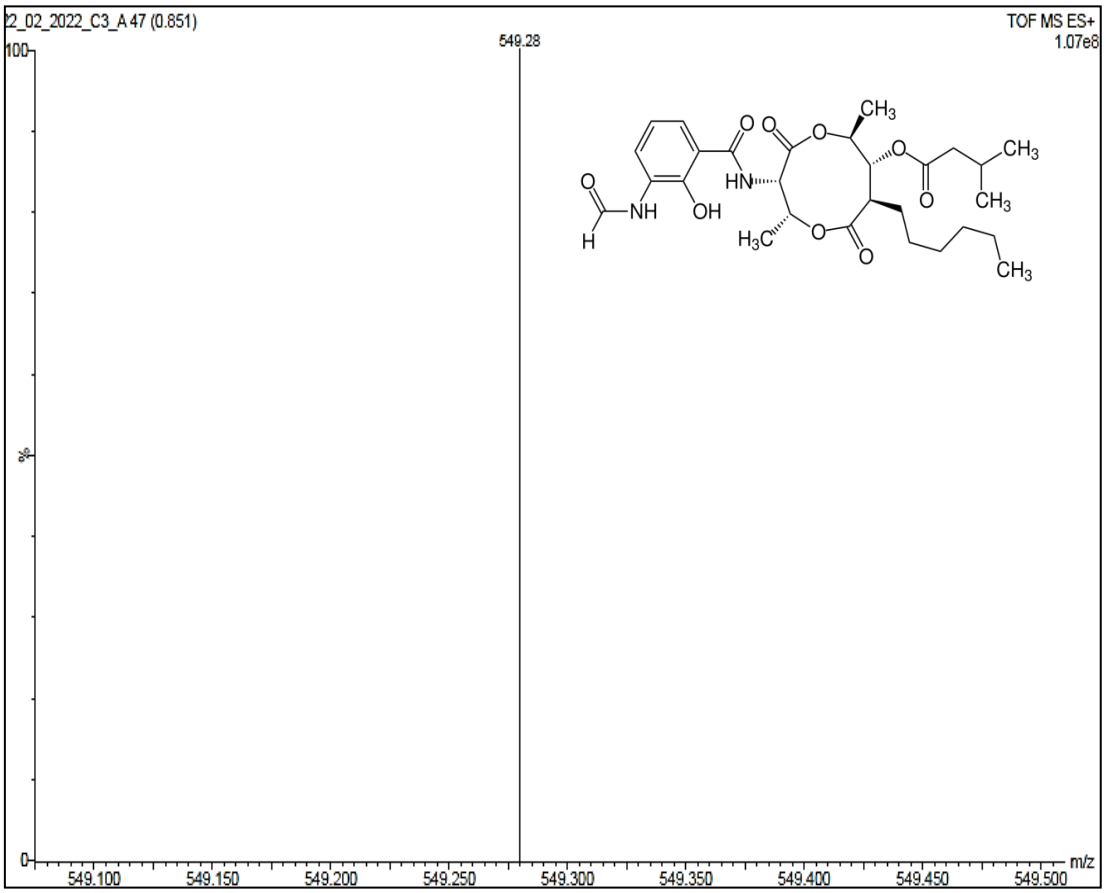

Fig. 8. LC-MS analysis of Antimycin A

Observations for the UV spectrum of fraction F3 (compound 2) recorded peaks at 227, 230, and 231 nm (Fig. 9A). The FT-IR spectrum showed an acidic stretching peak at 3386 cm^{-1}, indicating the presence of -OH group of carboxylic acid. Peaks at 1675 and 1594 cm^{-1} specified the presence of C=O stretching and -OH stretching in phenol group, respectively (Fig. 9B).

The ^{1}H NMR spectra of the compound 2 projects the following: peaks at 6.808 to 6.829 ppm (2H, d, Ar-H) due to aromatic protons, at 7.776 to 7.799 ppm (2H, d, Ar-H), in the downfield 10.214 ppm (1H, s, -OH) and 12.417 ppm (1H, s, -COOH) were observed. Peaks between 2 to 4 ppm indicate the presence of alkene protons. Similarly, it was observed that the ^{13}C NMR spectra showed downfield carbon signals at 115.586 ppm in the aromatic region (meta position) and at 121.855 ppm in the para position. The peak at 131.994 ppm signifies C=O group, *i.e.*, carbon of aromatic ring close to the carboxylic acid. The C-O of (OH) phenolic group was illustrated at 162.060 ppm and finally at 167.636 ppm (C=O) a carboxylic acid was shown. The other carbon signals were in the upfield region from 39.418 to 40.420 ppm (Fig. 10A and 10B). The mass spectrum showed an M^{+} ion peak at 139 amu and therefore it clearly revealed that the compound was 4-hydroxybenzoic acid with a molecular weight of 139.04 g/mol and molecular formula of $C_7H_6O_3$ (Fig. 11).

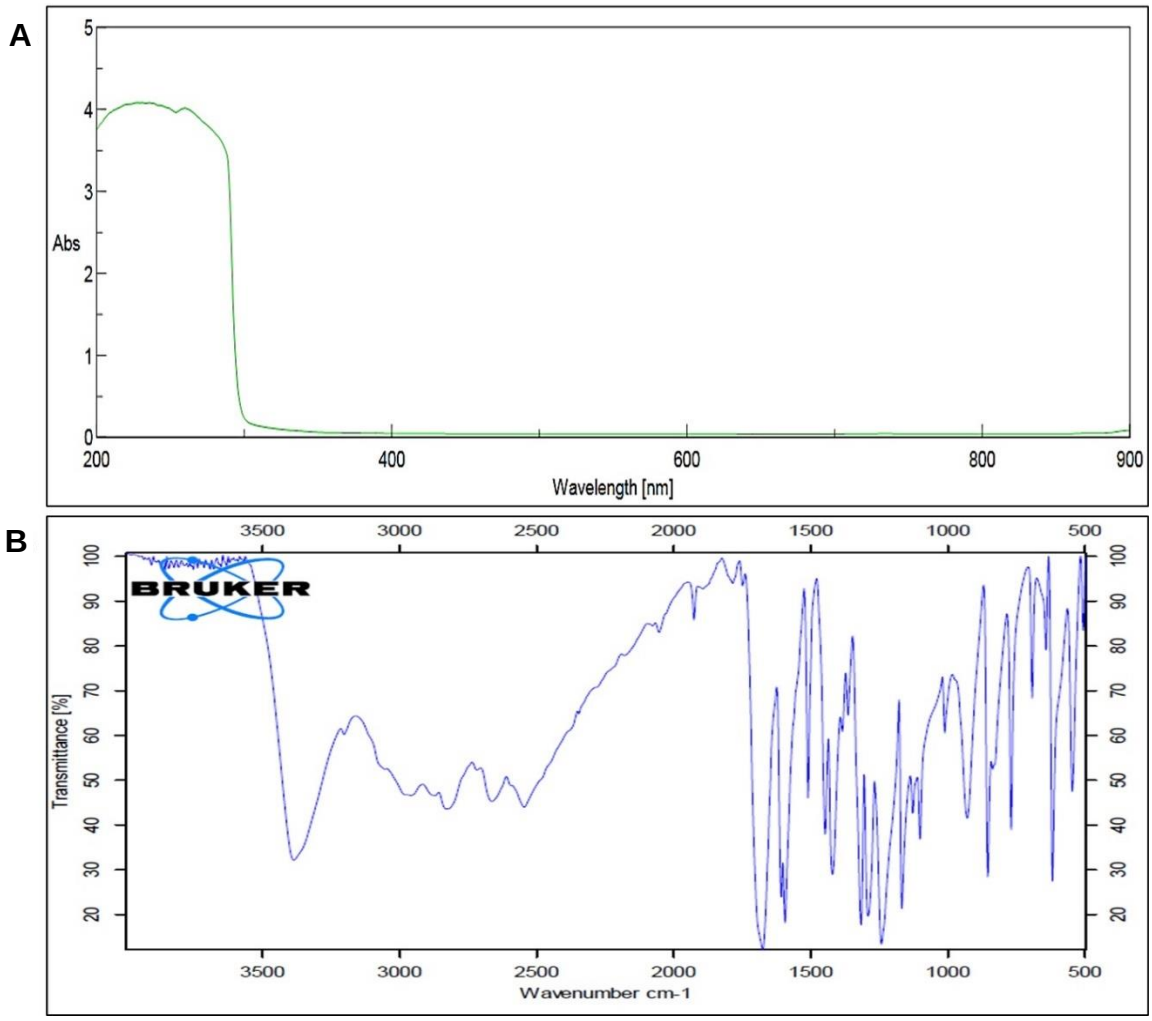

Fig. 9. A) UV visible spectroscopy and B) FT-IR spectroscopy of 4-hydroxybenzoic acid

4-hydroxybenzoic acid and its esterified forms are a well-known preservative in cosmetics, pharmaceuticals, and food industries. This compound continues to add other biological traits such as antibacterial, antiviral, antioxidant, anti-inflammatory, and hypoglycemic properties. In industries, its manufacturing parameters require high temperature and high-pressure conditions, with an addition of toxic catalysts. Therefore, the present way of producing the compounds by cultivating microbes in large quantities and extraction adds advantage over chemical synthesis (Maki and Takeda 2000). In bacteria, 4-hydroxybenzoic acid naturally occurs as a precursor for ubiquinone synthesis (Barker and Frost 2001). In this context, strain LC-9 naturally produced the compound 4-hydroxybenzoic acid with potential antimicrobial and antioxidant activities.

Apoptosis and Cytotoxicity Assay

The apoptosis and cytotoxicity effect of Antimycin A (Fig. 12) and 4-hydroxybenzoic acid (Fig. 13) were studied against MCF-7 cancer cell lines. Antimycin A and 4-hydroxybenzoic acid showed 30 to 95% of cell viability compared to the standard (20 to 97%). The IC_{50} values for Antimycin A and 4-hydroxybenzoic acid were found to be 9.6 ± 0.7 and 20.8 ± 0.4 µg/mL, respectively. The standard (Doxorubicin) showed IC_{50} value of 7.6 ± 1.3 µg/mL.

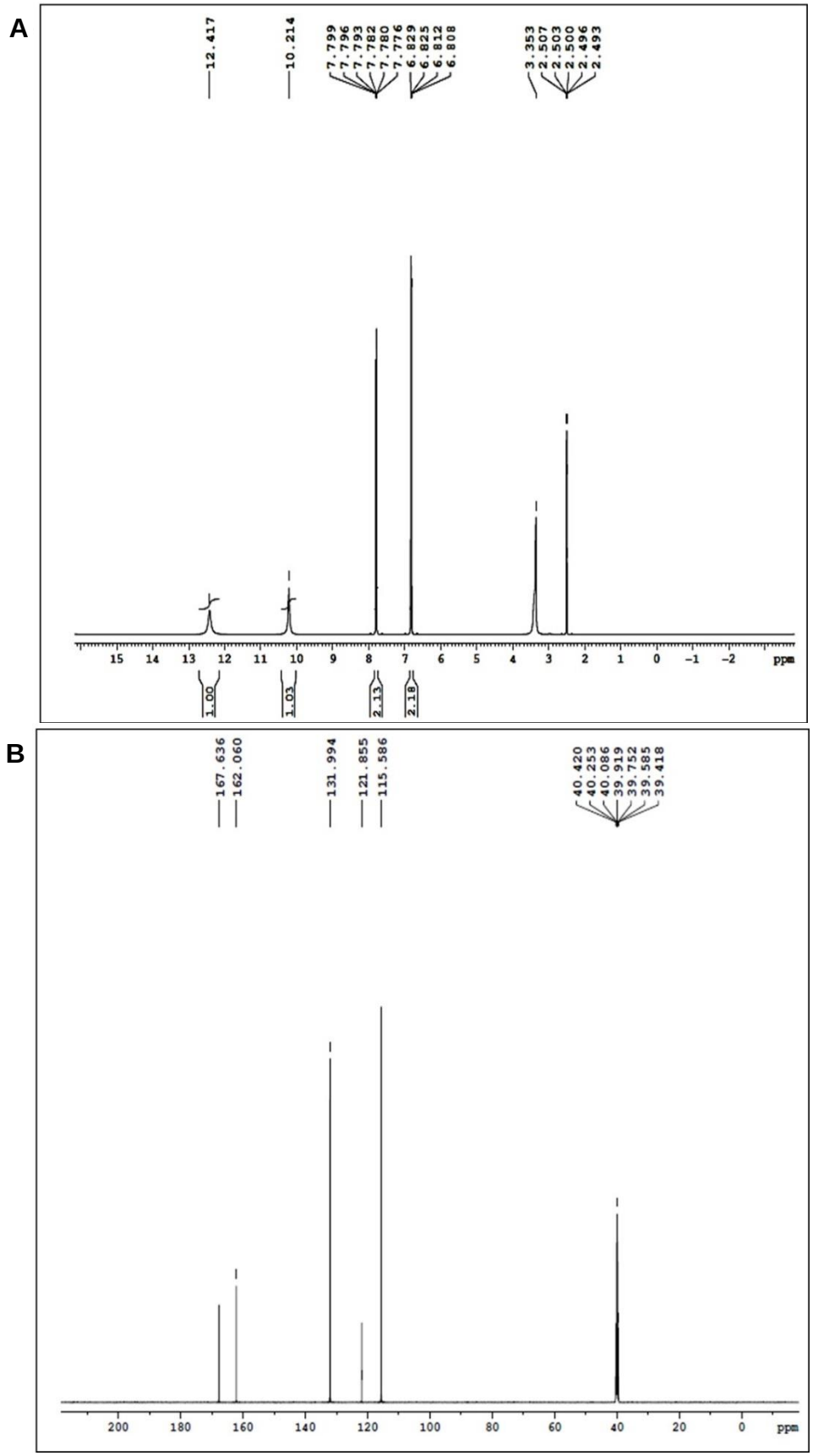
A
12.417
10.214
7.799
7.796
7.793
7.782
7.780
7.776
6.829
6.825
6.812
6.808
3.353
2.507
2.503
2.500
2.496
2.493
15 14 13 12 11 10 9 8 7 6 5 4 3 2 1 0 −1 −2 ppm
1.00
1.03
2.13
2.18
B
167.636
162.060
131.994
121.855
115.586
40.420
40.253
40.086
39.919
39.752
39.585
39.418
200 180 160 140 120 100 80 60 40 20 0 ppm

Fig. 10. A) ^{1}H NMR spectrum and B) ^{13}C NMR spectrum of 4-hydroxybenzoic acid

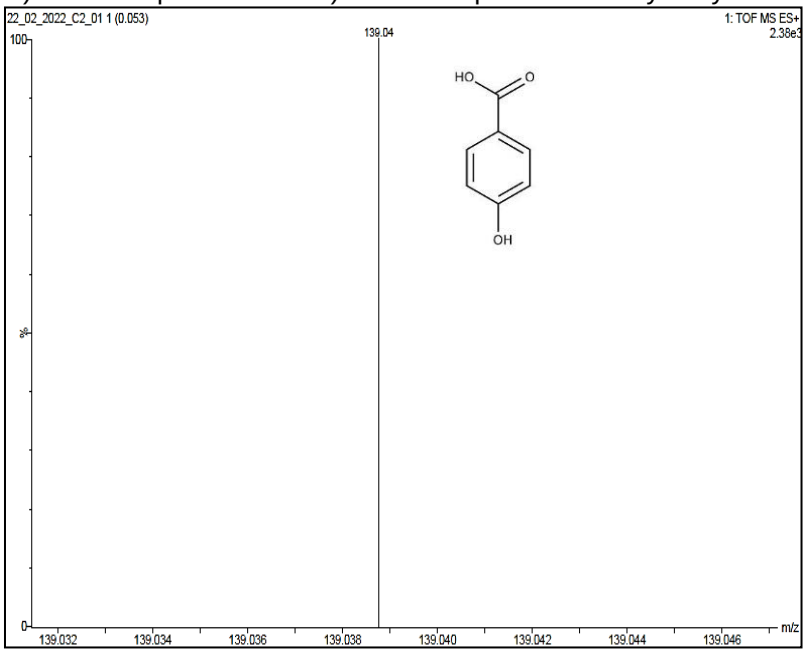

Fig. 11. LC-MS analysis of 4-hydroxybenzoic acid

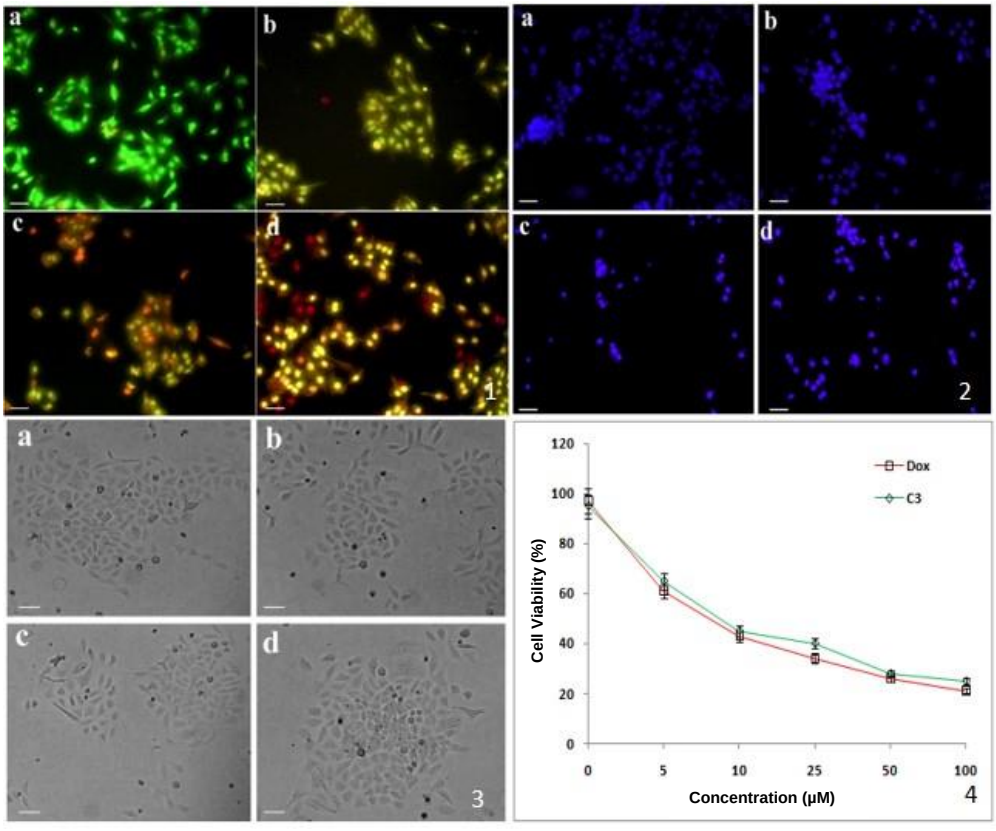

Fig. 12. Apoptosis and cytotoxicity assay of Antimycin A
1) AO/EtBr staining of MCF-7 cells treated with Antimycin A
2) DAPI staining of MCF-7 cells treated with Antimycin A
3) Antimycin A-treated MCF-7 cancer cells (MTT assay)
4) Cytotoxicity of Antimycin A and Doxorubicin at varied concentrations.

a) Control (Untreated), b) 10 µM-treated cells, c) 25 µM-treated cells, and d) 50 µM-treated cells

The cell morphology was observed for the MCF-7 apoptotic and necrotic cells by fluorescence microscopy upon treatment with the extracted compounds. In AO/EtBr staining method, the orange colour indicated apoptotic bodies, the red colour denoted cell necrosis, and the green colour was the reference of untreated samples with viable cells. The colouring pattern was a tool to identify apoptosis-associated changes in cell membranes. Similarly, after DAPI staining, the sample excited blue fluorescence.

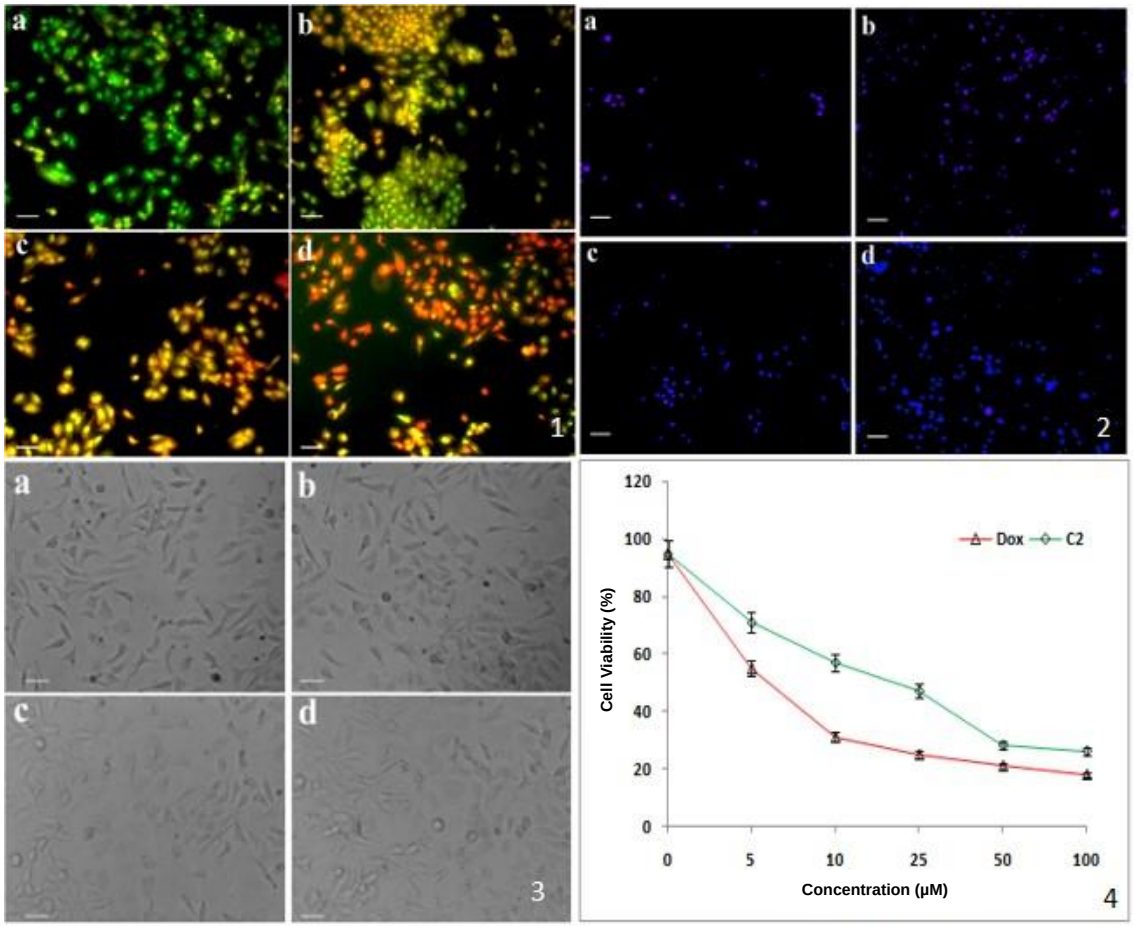

Fig. 13. Apoptosis and cytotoxicity assay of 4-hydroxybenzoic acid
1) AO/EtBr staining of MCF-7 cells treated with 4-hydroxybenzoic acid
2) DAPI staining of MCF-7 cells treated with 4-hydroxybenzoic acid
3) 4-hydroxybenzoic acid-treated MCF-7 cancer cells (MTT assay)
4) Cytotoxicity of 4-hydroxybenzoic acid and Doxorubicin at varied concentrations
a) Control (Untreated), b) 10 µM-treated cells, c) 25 µM-treated cells, and d) 50 µM-treated cells

Amongst actinomycetes, members of *Nocardiopsis* have been recently identified as excellent producers of bioactive metabolites (Shady *et al*. 2022). Additionally, it was found that the major cytotoxic compounds belong to the class dilactones. Antimycin analogues are dilactones naturally present in *Streptomyces* sp. and the metabolite is produced by actinomycetes from different origins (soil, marine, *etc.*). Subsequently, the anticancer property of antimycin have been tested for lung cancer, breast cancer, and glioblastoma cells for cytotoxic effects (Quinn *et al*. 2020). In this investigation, the compounds Antimycin A and 4-hydroxybenzoic acid were tested for cytotoxic activity against MCF-7

cell lines. The findings indicated that the assays employed in the study were well known for screening anticancer agents with cytotoxic activities.

Molecular Docking and ADME Analysis

Several drug targets have been identified for microbial activity from varying pathogens and targets of the cancers remain in the onset of discovery (Parasuraman *et al*. 2014; Pundarikakshudu and Kanaki 2019; Khusro *et al*. 2020). In the present study, known drug targets with credential and validation were selected to determine the interaction of the protein and the compounds of the study. Therefore, the small molecules identified from strain LC-9, *i.e.* Antimycin A and 4-hydroxybenzoic acid were screened computationally against the bacterial, fungal, and cancer targets.

Antimycin A showed maximum docking scores of -7.122 and -9.111 kcal/mol against N-myristoyl transferase and 14-α-demethylase antifungal targets, respectively. The active site residue interactions and the hydrogen bond distance were measured and summarized (Table 3). Among different targets of bacteria, a docking score of -5.881 kcal/mol was reported against isoleucyl-tRNA synthetase. Similarly, the compound showed a docking score of -6.243 kcal/mol against HER2-human epidermal growth factor receptor 2 (Fig. 14).

Table 3. Docking Analysis of Antimycin A against the Target Proteins of Bacteria, Fungi, and MCF-7 Cancer Cell Line

PDB ID	Docking Score	Glide g-Score	Glide Energy	Glide e-Model	Interacting Residues	H-bond Distance
Antifungal						
1IYL	-7.122	-7.178	-47.341	-57.657	ASP 412 GLY 413 TYR 225 TYR 354	2.11 2.40 1.89 2.30
5FSA	-9.111	-9.167	-55.933	-79.387	PRO 462 PRO 462 TYR 132 TYR 132	1.73 1.70 1.97 1.92
Antibacterial						
2VEG	-3.972	-4.028	-47.479	-53.478	LYS 237 MET 135	2.17 2.63
1ILE	-5.881	-5.937	-50.529	-68.54	LYS 25 GLN 28 ASP 142	2.57 1.82 1.99
2RJG	-3.374	-3.43	-41.962	-47.706	LYS 339	2.43
3UDI	-3.932	-3.99	-41.56	-49.66	LYS 255	1.9
Anticancer						
5VAX	-2.77	-2.826	-42.829	-45.789	ARG A12	2.6
1ZXM	-3.883	-3.939	-39.163	-42.509	THR 147	2.27
5O4G	-6.243	-6.299	-60.386	-79.287	GLU A165 SER A165 PRO A40 PRO A40	2.06 2.60 2.34 1.91
2J6M	-3.259	-3.315	-40.918	-49.126	NA	NA

NA: Not available

4-hydroxybenzoic acid exhibited binding energy values of -5.171, -6.218, -6.851, 6.322, -7.095, and -9.567 kcal/mol against N-myristoyl transferase, isoleucyl-tRNA synthetase, alanine racemase, dihydrofolate reductase, vascular endothelial growth factor receptor 2, and DNA topoisomerases II, respectively (Table 4 and Fig. 15).

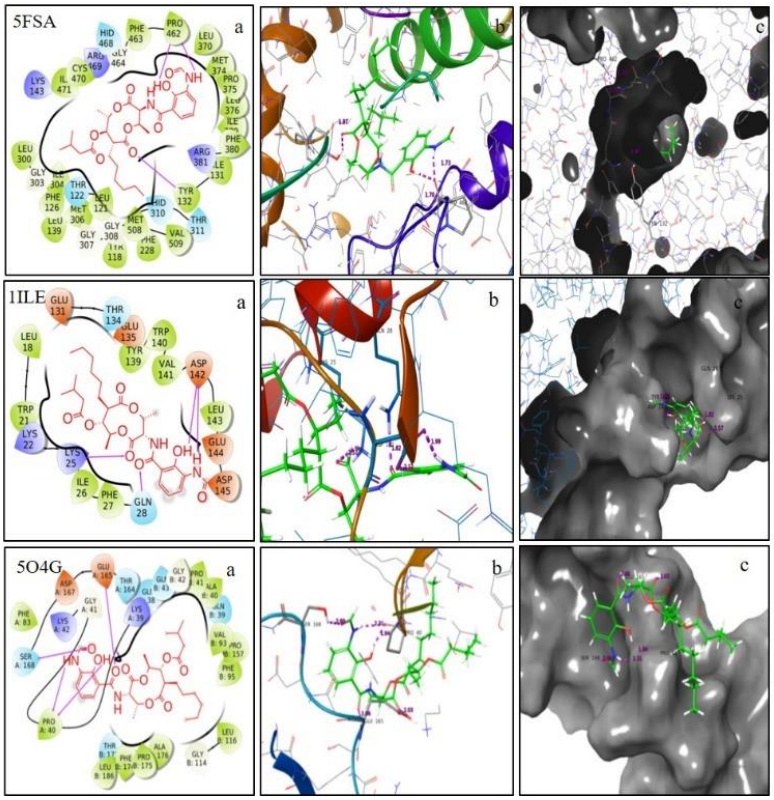

Fig. 14. Best binding mode and hydrogen bond interactions of Antimycin A with binding pockets of antifungal target (PDB ID: 5FSA), antibacterial target (PDB ID: 1ILE), anticancer target (PDB ID: 5O4G): a, b, and c represent 2D interactions, 3D interactions, and docked poses, respectively

Table 4. Docking Analysis of 4-hydroxybenzoic Acid Against Target Proteins of Bacteria, Fungi, and MCF-7 Cancer Cell Line

PDB ID	Docking Score	Glide g-Score	Glide Energy	Glide e-Model	Interacting Residues	H-bond Distance
Antifungal						
1IYL	-5.171	-5.171	-20.577	-27.217	LEU 450	1.99
5FSA	-4.229	-4.229	-19.824	-22.443	THR 315, PRO 462	2.06, 1.98
Antibacterial						
2VEG	-5.125	-5.125	-18.645	-30.746	ARG 282, LYS 237, ASN 17	1.83, 1.72, 2.14
1ILE	-6.218	-6.218	-20.315	-32.705	VAL 141	1.68
2RJG	-6.851	-6.851	-21.604	-27.306	ALA 342	1.91
3UDI	-4.934	-4.934	-19.24	-27.72	PHE 554	1.84
3SRW	-6.322	-6.322	-22.303	-32.964	THR 47, ALA 8	2.18, 1.95
Anticancer						
5EW3	-7.095	-7.095	-23.063	-36.823	ASP 1046, CYS 919	2.66, 2.18
5VAX	-5.969	-5.969	-15.182	-22.235	ASP 171, ARG D12	1.80, 1.84
1ZXM	-9.567	-9.567	-37.996	-93.422	ALA 167	2.04
5O4G	-5.508	-5.508	-23.663	-42.368	ALA 43, LYS 39, LYS 45	1.70, 1.80, 2.21
2J6M	-6.152	-6.152	-21.876	-30.332	MET 793	2.04

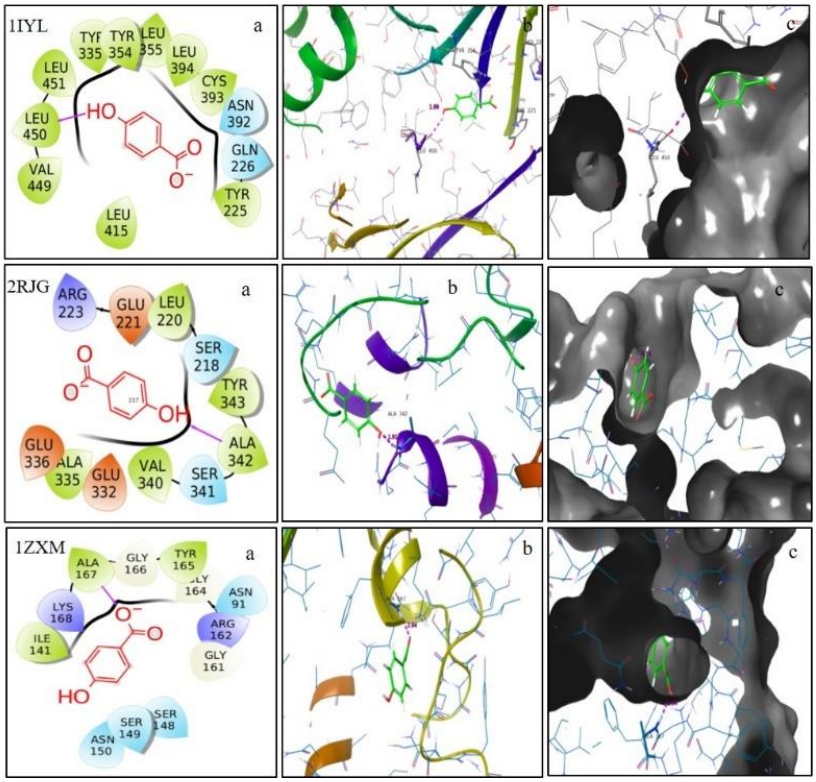

Fig. 15. Best binding mode and hydrogen bond interactions of 4-hydroxybenzoic acid with binding pockets of antifungal target (PDB ID: 1IYL), antibacterial target (PDB ID: 2RJG), anticancer target (PDB ID: 1ZXM): a, b, and c represent 2D i, 3D interactions, and docked poses, respectively

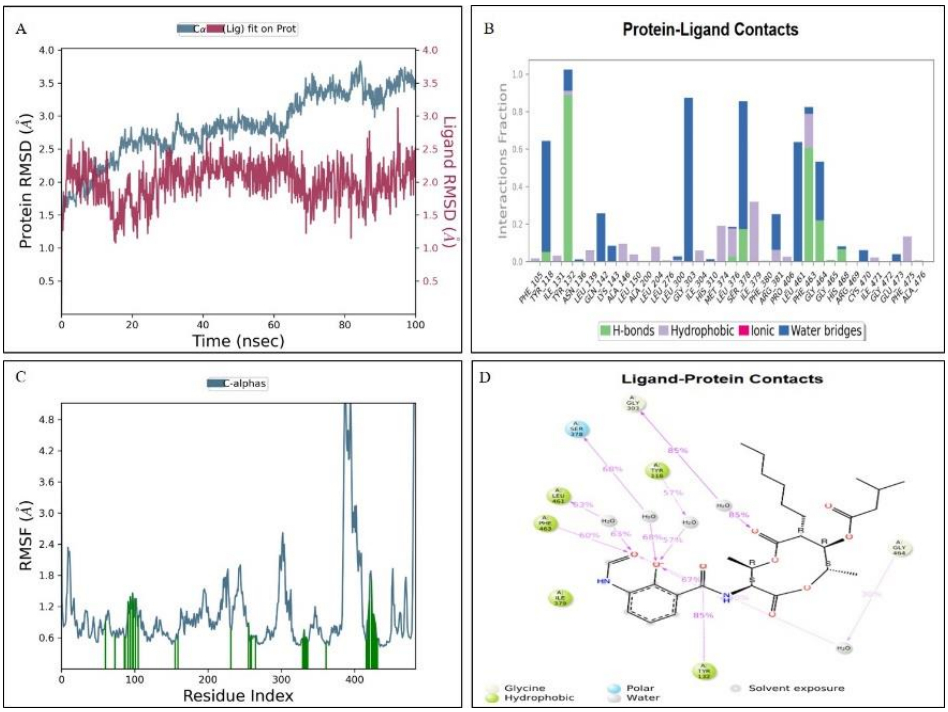

Fig. 16. (A) RMSD and (B) RMSF plot of protein 5FSA and Antimycin A during 100 ns MD trajectory. (C) The hydrogen, hydrophobic, and water bridges of Antimycin A with respect to residues of 5FSA during 100 ns MD simulation. (D) Two-dimensional interaction of Antimycin A-5FSA complex

Both compounds were evaluated for ADME properties, and the results are summarized in Table 6. The current research focus intends to encompass the information on target proteins and the mechanism of action of selected metabolites for therapeutic purposes. Antimycin A proved to have better binding efficiency as inhibitors of fungal proteins. Meanwhile, 4-hydroxybenzoic acid showed higher values for microbial targets, including dihydropteroate synthetase, isoleucyl-tRNA synthetase, alanine racemase, penicillin-binding protein, and dihydrofolate reductase. These targets involved in the study include regulators that create changes in DNA structure, modify DNA replication, and alter transcription, recombination, and chromatin remodeling mechanisms (Kumar *et al*. 2018; Crisci *et al*. 2019).

Molecular Dynamics

Antimycin A exhibited the highest interaction energy with the antifungal protein 14-α-demethylase. Both RMSD and RMSF plots were presented, and ligand-protein contacts showed hydrophobic interaction of 85% of the simulated time in the trajectory (Fig. 16).

4-Hydroxybenzoic acid possessed the highest docking score with the cancer target DNA topoisomerases II. The hydrogen bond interactions of 4-hydroxybenzoic acid with respect to residues of 1ZXM (OH-ASN 95) presented 43% of the simulated time in the trajectory (Fig. 17).

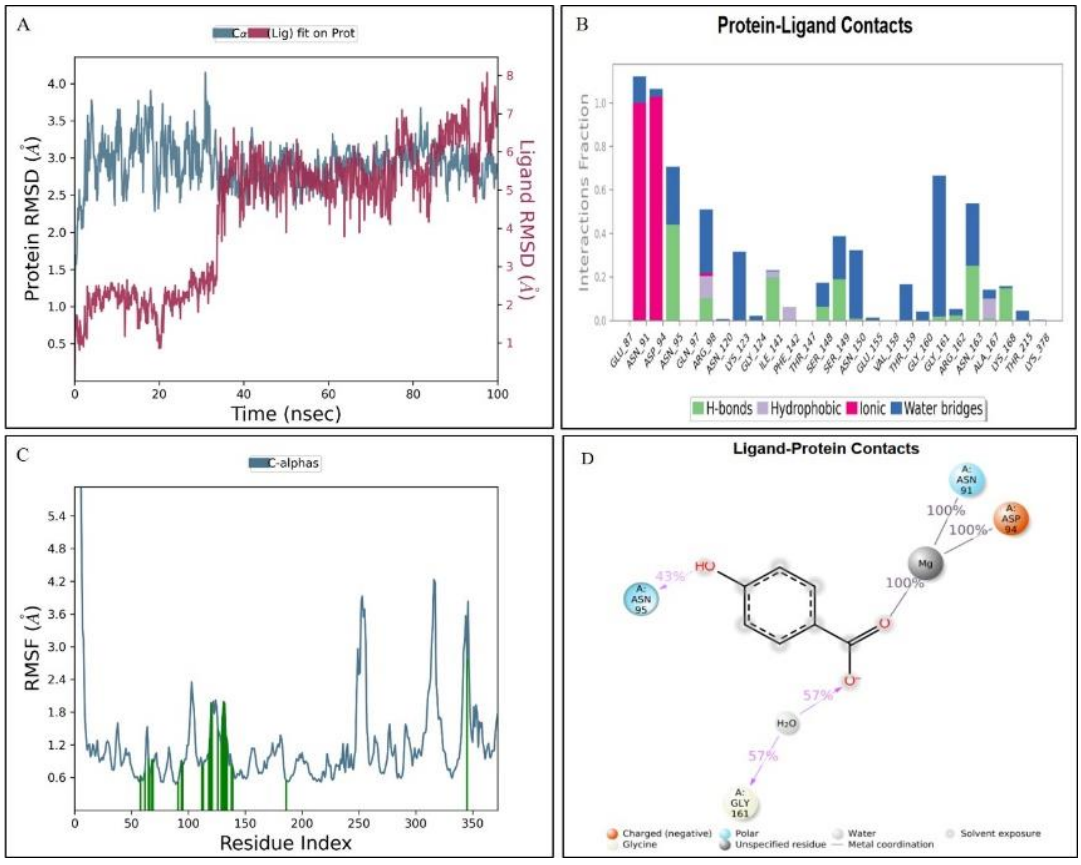

Fig. 17. (A) RMSD and (B) RMSF plot of protein 1ZXM and 4-hydroxybenzoic acid during 100 ns MD trajectory. (C) The hydrogen, hydrophobic, and water bridges of 4-hydroxybenzoic acid with respect to residues of 1ZXM during 100 ns MD simulation. (D) Two-dimensional interaction of 4-hydroxybenzoic acid-1ZXM complex

CONCLUSIONS

1. Bioactive compounds (Antimycin A and 4-hydroxybenzoic acid) were isolated from *Nocardiopsis* sp. strain LC-9.
2. Antimycin A and 4-hydroxybenzoic acid showed potential antimicrobial activities against bacterial and fungal pathogens.
3. Both compounds exhibited antioxidant activities with prominent IC_{50} values.
4. Antimycin A and 4-hydroxybenzoic acid revealed anticancer activities against MCF-7 cancer cells with an IC_{50} value of 9.6 ± 0.7 and 20.8 ± 0.4 µg/mL, respectively.
5. Antimycin A and 4-hydroxybenzoic acid showed remarkable interaction with microbial and cancer targeted proteins, thereby confirming the pharmaceutical efficacy of these compounds.

ACKNOWLEDGMENTS

Authors are grateful to Researchers Supporting Project number (RSP2024R414), King Saud University, Riyadh, Saudi Arabia. UV-Vis spectrophotometer and ATR-FT-IR Spectroscopy were utilized from DST-FIST instrumentation centre, Stella Maris College, Chennai. The instrumentation facility for NMR and LC-MS was procured from SAIF IITM.

REFERENCES CITED

Abdel-Razek, A. S., El-Naggar, M. E., Allam, A., Morsy, O. M., and Othman, S. I. (2020). "Microbial natural products in drug discovery," *Processes* 8(4), article 470. DOI: 10.3390/pr8040470

Barker, J. L., and Frost, J. W. (2001). "Microbial synthesis of p-hydroxybenzoic acid from glucose," *Biotechnology and Bioengineering* 76(4), 376-390. DOI: 10.1002/bit.10160

Benzie, I. F., and Strain, J. J. (1996). "The ferric reducing ability of plasma (FRAP) as a measure of antioxidant power: The FRAP assay," *Analytical Biochemistry* 239(1), 70-76.

Clarance, P., Luvankar, B., Sales, J., Khusro, A., Agastian, P., Tack, J. C., Al-Khulaifi, M. M., Al-Shwaiman, H. A., Elgorban, A. M., Syed, A., *et al.* (2020). "Green synthesis and characterization of gold nanoparticles using endophytic fungi *Fusarium solani* and its *in-vitro* anticancer and biomedical applications," *Saudi Journal of Biological Sciences* 27, 706-712. DOI: 10.1016/j.sjbs.2019.12.026

Crisci, S., Amitrano, F., Saggese, M., Muto, T., Sarno, S., Mele, S., Vitale, P., Ronga, G., Berretta, M., and Di Francia, R. (2019). "Overview of current targeted anti-cancer drugs for therapy in onco-hematology," *Medicina* 55(8), article 414. DOI: 10.3390/medicina55080414

Dror, B., Jurkevitch, E., and Cytryn, E. (2020). "State-of-the-art methodologies to identify antimicrobial secondary metabolites in soil bacterial communities – A review," *Soil Biology and Biochemistry* 147, article ID 107838. DOI: 10.1016/j.soilbio.2020.107838

Goel, N., Fatima, S. W., Kumar, S., Sinha, R., and Khare, S. K. (2021). "Antimicrobial resistance in biofilms: Exploring marine actinobacteria as a potential source of antibiotics and biofilm inhibitors," *Biotechnology Reports* 30, article e00613. DOI: 10.1016/j.btre.2021.e00613

Han, Z., Xu, Y., McConnell, O., Liu, L., Li, Y., Qi, S., Huang, X., and Qian, P. (2012). "Two antimycin A analogues from marine-derived actinomycete *Streptomyces lusitanus*," *Marine Drugs* 10(3), 668-676. DOI: 10.3390/md10030668

Hauhan, J. V., and Gohel, S. D. (2020). "Molecular diversity and pharmaceutical applications of free-living and Rhizospheric marine Actinobacteria," in: *Marine Niche: Applications in Pharmaceutical Sciences*, Springer, Singapore, pp. 111-131.

Hytti, M., Korhonen, E., Hyttinen, J. M. T., Roehrich, H., Kaarniranta, K., Ferrington, D. A., and Kauppinen, A. (2019). "Antimycin A-induced mitochondrial damage causes human RPE cell death despite activation of autophagy," *Oxidative Medicine and Cellular Longevity* 2019, article ID 1583656. DOI: 10.1155/2019/1583656

Imamura, N., Nishijima, M., Adachi, K., and Sano, H. (1993). "Novel antimycin antibiotics, urauchimycins A and B, produced by marine actinomycete," *The Journal of Antibiotics* 46(2), 241-246. DOI: 10.7164/antibiotics.46.241

Jia, Z.-S., Tang, M.-C., and Wu, J.-M. (1999). "The determination of flavonoid contents in mulberry and their scavenging effects on superoxide radicals," *Food Chemistry* 64(4), 555-559. DOI: 10.1016/s0308-8146(98)00102-2

Kauppinen, A. (2018). "Mitochondria-associated inflammasome activation and its impact on aging and age-related diseases," in: *Handbook of Immunosenescence*, T. Fulop, C. Franceschi, K. Hirokawa, G. Pawelec, (eds.), Springer, Cham, Switzerland, pp. 1-20. DOI: 10.1007/978-3-319-64597-1_107-1

Kekuda, T., Shobha, K. S., and Onkarappa, R. (2010). "Studies on antioxidant and antihelmintic activity of two *Streptomyces* species isolated from Western Ghat soils of Agumbe, Karnataka," *Karnataka Journal of Pharmaceutical Research*, 3, 26-29.

Khusro, A., Aarti, C., and Agastian, P. (2020). "Computational modelling and docking insight of bacterial peptide as ideal anti-tubercular and anticancer agents," *Biocatalysis and Agricultural Biotechnology* 26, article ID 101644. DOI: 10.1016/j.bcab.2020.101644

Kumar, B., Singh, S., Skvortsova, I., and Kumar, V. (2018). "Promising targets in anti-cancer drug development: Recent updates," *Current Medicinal Chemistry* 24(42), 4729-4752. DOI: 10.2174/0929867324666170331123648

Kumar, K. D., Vigneshwari, J., Gnanasekaran, A., Selvamani, V., and Senthilkumar, P. (2023). "Multipotential secondary metabolites from *Nocardiopsis dassonovillei* of marine Actinomycetes and their *in silico* studies," *Bioscience Biotechnology Research Asia* 20(1), 173-187. DOI: 10.13005/bbra/3079

Maki, T., and Takeda, K. (2000). "Benzoic acid and derivatives," *Ullmann's Encyclopedia of Industrial Chemistry* 3, pp, 329-342.

Mosmann, T. (1983). "Rapid colorimetric assay for cellular grow and survival: Application to proliferation and cytotoxicity assays," *Journal of Immunological Methods* 65, 55-63. DOI: 10.1016/0022-1759(83)90303-4

Ngema, S. S., Khumalo, S. H., Ojo, M. C., Pooe, O. J., Malilehe, T. S., Basson, A. K., and Madoroba, E. (2023). "Evaluation of antimicrobial activity by marine *Nocardiopsis dassonvillei* against foodborne *Listeria monocytogenes* and Shiga toxin-producing *Escherichia coli*," *Microorganisms* 11(10), article 2539. DOI: 10.3390/microorganisms11102539

Oyaizu, M. (1986). "Studies on product of browning reaction prepared from glucose amine," *Japanese Journal of Nutrition* 44, 307-315.

Parasuraman, S., Thing, G., and Dhanaraj, S. (2014). "Polyherbal formulation: Concept of ayurveda," *Pharmacognosy Reviews* 8(16), 73-80. DOI: 10.4103/0973-7847.134229

Prasathkumar, M., Raja, K., Vasanth, K., Khusro, A., Sadhasivam, S., Sahibzada, M. U. K., Gawwad, M. R. A., Al Farraj, D. A., and Elshikh, M. S. (2021). "Phytochemical screening and *in vitro* antibacterial, antioxidant, anti-inflammatory, anti-diabetic, and wound healing attributes of *Senna auriculata* (L.) Roxb. Leaves," *Arabian Journal of Chemistry* 14, article ID 103345. DOI: 10.1016/j.arabjc.2021.103345

Pundarikakshudu, K., and Kanaki, N. S. (2019). "Analysis and regulation of traditional Indian medicines (TIM)," *Journal of AOAC International* 102(4), 977-978. DOI: 10.5740/jaoacint.18-0376

Quinn, G. A., Banat, A. M., Abdelhameed, A. M., and Banat, I. M. (2020). "*Streptomyces* from traditional medicine: Sources of new innovations in antibiotic discovery," *Journal of Medical Microbiology* 69(8), 1040-1048. DOI: 10.1099/jmm.0.001232

Ramalingam, V., Rajaram, R., Archunan, G., Padmanabhan, P., and Gulyás, B. (2022). "Structural characterization, antimicrobial, antibiofilm, antioxidant, anticancer and acute toxicity properties of N-(2-hydroxyphenyl)-2-phenazinamine from *Nocardiopsis exhalans* (KP149558)," *Frontiers in Cellular and Infection Microbiology* 12, article ID 794338. DOI: 10.3389/fcimb.2022.794338

Salwan, R., and Sharma, V. (2020). "Molecular and biotechnological aspects of secondary metabolites in actinobacteria," *Microbiological Research* 231, article ID 126374. DOI: 10.1016/j.micres.2019.126374

Saraswathi, K., Mahalakshmi, S., Khusro, A., Arumugam, P., Al Farraj, D. A., and Alkufeidy, R. M. (2020). "*In vitro* biological properties of *Streptomyces cangkringensis* isolated from the floral rhizosphere regions," *Saudi Journal of Biological Sciences* 27, 3249-3257. DOI: 10.1016/j.sjbs.2020.09.035

Selim, M. S. M., Abdelhamid, S. A., and Mohamed, S. S. (2021). "Secondary metabolites and biodiversity of actinomycetes," *Journal, Genetic Engineering & Biotechnology* 19(1), article 72. DOI: 10.1186/s43141-021-00156-9

Shady, N. H., Tawfike, A. F., Yahia, R., Fouad, M. A., Brachmann, A. O., Piel, J., Abdelmohsen, U. R., and Kamel, M. S. (2022). "Cytotoxic activity of actinomycetes *Nocardia* sp. and *Nocardiopsi*s sp. associated with marine sponge *Amphimedon* sp.," *Natural Product Research* 36(11), 2917-2922. DOI: 10.1080/14786419.2021.1931865

Siddharth, S., Aswathanarayan, J. B., Kuruburu, M. G., Madhunapantula, S. R. V., and Vittal, R. R. (2021). "Diketopiperazine derivative from marine actinomycetes *Nocardiopsis* sp. SCA30 with antimicrobial activity against MRSA," *Archives of Microbiology* 203(10), 6173-6181. DOI: 10.1007/s00203-021-02582-2

Venkatadri, B., Khusro, A., Aarti, C., Rameshkumar, M. R., and Agastian, P. (2017). "*In vitro* assessment on medicinal properties and chemical composition of *Michelia nilagirica* bark," *Asian Pacific Journal of Tropical Biomedicine* 7(9), 782-790. DOI: 10.1016/j.apjtb.2017.08.003

Article submitted: May 23, 2024; Peer review completed: June 26, 2024; Revised version received: July 8, 2024; Accepted: August 3, 2024; Published: August 28, 2024.
DOI: 10.15376/biores.19.4.7673-7697